Torsional and axial compressive properties of tibiotarsal bones of red-tailed hawks (*Buteo jamaicensis*)

Shannon M. Kerrigan VMD
Amy S. Kapatkin DVM, MS
Tanya C. Garcia MS
Duane A. Robinson DVM, PhD
David Sanchez-Migallon Guzman LV, MS
Susan M. Stover DVM, PhD

Received March 9, 2017.
Accepted July 12, 2017.

From the Veterinary Medical Teaching Hospital (Kerrigan) and Departments of Surgical and Radiological Sciences (Kapatkin, Robinson), Anatomy, Physiology and Cell Biology (Garcia, Stover), and Medicine and Epidemiology (Sanchez-Migallon Guzman), School of Veterinary Medicine, University of California-Davis, Davis, CA 95616. Dr. Kerrigan's present address is Vista Veterinary Specialists, 7425 Greenhaven Dr, Sacramento, CA 95831. Dr. Robinson's present address is BluePearl Specialty and Emergency Pet Hospital, 13240 Aurora Ave N, Seattle, WA 98133.

Address correspondence to Dr. Kapatkin (askapatkin@ucdavis.edu).

OBJECTIVE
To describe the torsional and axial compressive properties of tibiotarsal bones of red-tailed hawks (*Buteo jamaicensis*).

SAMPLE
16 cadaveric tibiotarsal bones from 8 red-tailed hawks.

PROCEDURES
1 tibiotarsal bone from each bird was randomly assigned to be tested in torsion, and the contralateral bone was tested in axial compression. Intact bones were monotonically loaded in either torsion (n = 8) or axial compression (8) to failure. Mechanical variables were derived from load-deformation curves. Fracture configurations were described. Effects of sex, limb side, and bone dimensions on mechanical properties were assessed with a mixed-model ANOVA. Correlations between equivalent torsional and compressive properties were determined.

RESULTS
Limb side and bone dimensions were not associated with any mechanical property. During compression tests, mean ultimate cumulative energy and postyield energy for female bones were significantly greater than those for male bones. All 8 bones developed a spiral diaphyseal fracture and a metaphyseal fissure or fracture during torsional tests. During compression tests, all bones developed a crushed metaphysis and a fissure or comminuted fracture of the diaphysis. Positive correlations were apparent between most yield and ultimate torsional and compressive properties.

CONCLUSIONS AND CLINICAL RELEVANCE
The torsional and axial compressive properties of tibiotarsal bones described in this study can be used as a reference for investigations into fixation methods for tibiotarsal fractures in red-tailed hawks. Although the comminuted and spiral diaphyseal fractures induced in this study were consistent with those observed in clinical practice, the metaphyseal disruption observed was not and warrants further research. (*Am J Vet Res* 2018;79:388–396)

Little information is available regarding the static mechanical properties of avian bones. Compared with the bones of other species, the bones of birds have a higher calcium content, which might contribute to brittleness, and some of the most frequently fractured bones of birds have scant soft tissue coverage.[1] Those characteristics often result in open, comminuted fractures that have a high risk of nonunion or infection after repair and contribute to the complexity of fracture repair in birds. Although many techniques commonly used in small animal fracture repair can be used to repair fractures in birds, modifications are required to account for the unique characteristics of avian bones and facilitate fracture stabilization compatible with a successful outcome.[1–4]

ABBREVIATIONS
PMMA Polymethylmethacrylate

The tibiotarsal bone, a long bone of the pelvic limb, is one of the most commonly fractured bones in birds.[1–4] Causes of tibiotarsal bone fractures include falling from a perch, being stepped on, unknown trauma, or, in the case of falconry, inadvertent application of force on the bone by the jess, or leg strap, during training of juvenile and inexperienced birds. Successful repair of any fractured bone requires excellent alignment of the fractured pieces, stability across the fractured surface and surrounding soft tissue, and an adequate blood supply. Specific to the tibiotarsal bone, successful fracture repair will facilitate a rapid return to function (eg, weight bearing), which is crucial for both the survival of the bird and its ability to function normally in its natural habitat. Raptors, such as red-tailed hawks (*Buteo jamaicensis*), also rely on their pelvic limbs for apprehension of food in the wild. A poorly functioning or malaligned tibiotarsal bone can result in an inability to capture prey

in the wild and death or prevent the bird from being released back to its natural habitat. It can also lead to asymmetric weight bearing and predispose the bird to diseases such as pododermatitis and bumblefoot.[1,4]

The purpose of the study reported here was to describe the axial compressive and torsional mechanical properties of the tibiotarsal bones of red-tailed hawks. We hypothesized that the torsional properties of those bones would be positively correlated with their compressive properties.

Materials and Methods

Specimen collection and preparation

Tibiotarsal bones (n = 16) obtained from 8 skeletally mature, apparently healthy red-tailed hawks that were euthanized for reasons unrelated to the study were evaluated. Immediately after euthanasia and confirmation of death, each bird was frozen and stored at –20°C until use. Sex and weight were recorded for each bird.

Within 72 hours prior to mechanical testing, each bird was allowed to thaw at room temperature (approx 22°C). Then, both tibiotarsal bones were harvested, wrapped in towels soaked with saline (0.9% NaCl) solution, and stored at –20°C until biomechanical testing. For each bird, 1 tibiotarsal bone was randomly assigned by means of a coin toss to be tested to failure in torsion, and the contralateral bone was assigned to be tested to failure in compression. The randomization protocol was designed such that 4 left and 4 right tibiotarsal bones would be tested to failure in torsion and in compression.

Craniocaudal and mediolateral radiographic images[a,b] were obtained (kVp, 48; mAs, 2) of all tibiotarsal bones before mechanical testing to rule out orthopedic disorders. Digital calipers[c] were used to measure tibiotarsal bone length and diaphyseal width on the radiographs. Bone length was measured from the tibial crest to the most distal aspect of the tibiotarsal-tarsometatarsal joint surface. Diaphyseal width (diameter) was measured at the middiaphyseal level in both craniocaudal and mediolateral orientations.

Mechanical testing

The proximal and distal aspects of each tibiotarsal bone were fixed in PMMA blocks.[d] The PMMA extended from the metaphyseal-epiphyseal junction to 1.5 cm past each end of the bone. The PMMA blocks were then mounted in a purpose-built alignment jig that was used to align the longitudinal axis of the bone with the center of rotation of a servohydraulic testing system.[e]

Each bone was loaded in either torsion at 5°/s in external rotation or axial compression at 2 mm/s. Both tests were performed under actuator displacement control. For the torsional test, the bone was axially loaded to 5 N (approx 50% of body weight), then axial actuator displacement was held constant while the bone was externally rotated to failure. Torque and angular actuator displacement (torsional test) or load and linear actuator displacement (compression test) data were acquired at 128 Hz throughout the test. For all tests, a video was recorded at 60 frames/s by each of 2 high-resolution (1,280 × 1,280 pixels) cameras.[f] For 1 set of bones (1 tested to failure in torsion and 1 tested to failure in compression), white dots were painted on the diaphysis, adjacent to the proximal and distal metaphyses, and on the PMMA blocks so that motion captured in the videos could be tracked by a motion analysis system[g] to better understand the local deformations that corresponded to the load-deformation data.

Craniocaudal and mediolateral radiographic images were obtained of all tibiotarsal bones after mechanical testing to document the fracture location and configuration. Fracture configurations were described for each bone. Then, the PMMA blocks were sawed in half so that the epiphyseal and metaphyseal regions of each bone could be examined.

Data reduction

For torsional tests, torque was plotted against angular actuator deformation. A first-yield point was noted when a sharp short decrease in torque was present at low torque (ie, 19% to 46% of maximum torque). The yield point was defined as the first gradual deviation in curve linearity at a higher torque than that at the first-yield point (when present), and when a first-yield point was not present, it was determined by a > 1% angular deformation offset between linear regression intercepts through consecutive data points. The ultimate point was defined as the point of maximum torque. The failure point was defined as the point of last recorded torque before bone fracture, which coincided with zero torque. Preyield stiffness was derived as the slope of the least squares linear regression line fit through the middle third of the data between the first-yield (ie, start of test) and yield points. Postyield stiffness was derived as the slope of the least squares linear regression line fit through the middle third of the data between the yield and ultimate points. First-yield, yield, ultimate, and failure torque and angle values were determined from the first-yield, yield, ultimate, and failure points, respectively. First-yield, yield, ultimate, and failure cumulative energies were calculated from the integral under the curve to the respective points. Postyield energy was calculated from the integral under the curve between the yield and ultimate points. Postultimate energy was calculated from the integral (Riemann sum by trapezoidal approximation) under the curve between ultimate and failure points.

For compressive tests, axial load was plotted against axial actuator displacement. A first-yield point was noted when a sharp, short decrease in force was present at low load (ie, 12% to 32% of maximum load). The yield point was determined in a manner similar to that used for torsional tests, with a > 0.1% axial displacement offset. The ultimate point was defined as the point of maximum load. The failure point was defined as the first point after maximum load, where

load decreased to 70% of maximum load. Stiffnesses and energies were calculated in the same manner as that used for torsional tests.

Statistical analysis

The data distribution for each of the mechanical properties of interest was assessed for normality by means of the Shapiro-Wilk test. For normally distributed variables, a mixed-model ANOVA[h] was used to identify factors associated with mechanical properties. Fixed effects included in the model were bird sex, limb side (left or right), and bone dimensions (bone length and diaphyseal diameter), and bird was included as a random effect to account for repeated measures within birds (ie, evaluation of both tibiotarsal bones). For each model, ANOVA residuals were assessed for normality by means of the Shapiro-Wilk test. For variables that were not normally distributed, the data were transformed to ranks, then an ANOVA was applied to the ranks. The respective correlations between torsional and compressive mechanical properties and between bone dimensions and mechanical properties were assessed by calculation of the Pearson correlation coefficient (r).[i] Values of $P \leq 0.05$ were considered significant for all analyses.

Results

Birds

The red-tailed hawks from which the tibiotarsal bones were obtained included 5 females (mean ± SD weight, 930.6 ± 82.2 g) and 3 males (mean ± SD weight, 964 ± 129.2 g). Mean bird weight (P = 0.584) and tibiotarsal bone dimensions ($P \geq 0.508$ for all comparisons) did not differ significantly between female and male bones. Limb side was not significantly ($P \geq 0.067$ for all comparisons) associated with any mechanical property and was not further considered.

Torsion

The mean ± SD bone length was 119.8 ± 4.9 mm for bones tested to failure in torsion **(Table 1)**. Bone length was not significantly associated with any torsional mechanical property. Diaphyseal diameter was not significantly ($P \geq 0.072$ for all comparisons) associated with any torsional mechanical property, and none of the torsional mechanical properties differed significantly ($P \geq 0.083$ for all comparisons) between female and male birds.

Data were normally distributed for all torsional mechanical properties except yield angle. One bone had yield, ultimate, and failure torques that were

Table 1—Dimensions and mechanical properties for 8 tibiotarsal bones obtained from red-tailed hawks (*Buteo jamaicensis*) that were tested to failure in torsion (torsional test).

Variable	No. of bones	Mean ± SD	Median (range)
Bone dimensions			
Diaphyseal craniocaudal diameter (mm)	8	7.1 ± 0.6	7.1 (5.8–7.8)
Diaphyseal mediolateral diameter (mm)	8	7.6 ± 0.8	7.6 (6.4–8.6)
Length (mm)	8	119.8 ± 4.9	122.4 (110.6–124.1)
First-yield point*			
Angle (°)	4	5.15 ± 1.70	5.07 (3.52–6.94)
Torque (N•mm)	4	882 ± 423	920 (417–1,269)
Stiffness (N•mm/°)	4	169.3 ± 20.5	170.8 (147.9–187.88)
Energy (N•mm•°)	4	2,705 ± 1,843	2,734 (805–4,549)
Yield point			
Angle (°)	8	17.7 ± 5.3	19.7 (5.0–20.96)
Torque (N•mm)	8	2,470 ± 1,019	2,709 (438–3,590)
Stiffness (N•mm/°)	8	133.7 ± 36.8	138.3 (84.2–180.3)
Cumulative energy (N•mm•°)	8	25,172 ± 11,864	26,354 (1,153–38,809)
Ultimate point			
Angle (°)	8	25.0 ± 8.9	26.2 (6.3–33.6)
Torque (N•mm)	8	2,958 ± 1,226	3,512 (465–4,066)
Postyield stiffness (N•mm/°)	7†	64.9 ± 46.5	76.1 (39.3–122.1)
Cumulative energy (N•mm•°)	8	47,428 ± 24,548	51,626 (1,760–74,475)
Postyield energy (N•mm•°)	8	22,256 ± 17,172	22,563 (607–45,618)
Failure point			
Displacement (°)	8	25.0 ± 8.92	26.2 (6.3–33.6)
Torque (N•mm)	8	2,958 ± 1,226	3,512 (465–4,066)
Cumulative energy (N•mm•°)	8	47,428 ± 24,548	51,626 (1,760–74,475)
Postultimate energy (N•mm•°)	8	0 ± 0	0 (0–0)

For each bird, 1 tibiotarsal bone was randomly assigned to be tested to failure in torsion, and the contralateral bone was assigned to be tested to failure in compression. The randomization protocol was designed such that 4 left and 4 right tibiotarsal bones would be tested to failure in torsion and in compression. Limb side was not significantly associated with any mechanical property; therefore, data for left and right tibiotarsal bones were combined for analyses. Each bone was loaded in torsion at 5°/s in external rotation under actuator displacement control and axially loaded to 5 N (approx 50% of body weight). Axial actuator displacement was held constant while the bone was externally rotated to failure, and torque and angular actuator displacement data were acquired at 128 Hz throughout the test. *Only 4 bones had a first-yield point. †One bone had a decrease in load between the ultimate and failure points that affected only postyield stiffness, so the datum for that bone was discarded for that variable.

< 18% of the corresponding mean torques for the other 7 bones. All bones failed at the ultimate (maximum) torque; thus, failure torque was the same as ultimate torque **(Figure 1)**. The mean axial compressive load induced by torsion was 56 N, which was 3.5% of the yield strength during axially compressive tests.

All bones tested in torsion failed with a spiral fracture configuration, which included the proximal half of the diaphysis **(Figure 2)**. Within the diaphysis, 4 bones had a comminuted spiral fracture, 3 bones had an incomplete spiral fracture, and 1 had a simple spiral fracture. All 8 bones had fissures that extended into the proximal metaphysis. Additionally, 3 bones had a fracture that extended into the proximal metaphysis, and 4 bones had a fracture that extended into the distal metaphysis. Two bones had fractures that extended into both the proximal and distal metaphyses. Examination of the video of the marked bone tested in torsion revealed that the distal metaphysis became displaced early in the test before spiral fracture of the diaphysis **(Figure 3)**. Only 4 bones had a first-yield point. None of the mechanical properties differed significantly between bones that did and did not have a first-yield point.

Compression

Although 8 bones were tested to failure in compression, there was a malfunction during the test for 1 bone; therefore, data from only 7 bones were analyzed. The mean ± SD bone length for bones tested in compression was 119.3 ± 5.1 mm **(Table 2)**. Neither bone length nor diameter was significantly ($P \geq 0.256$ for all comparisons) associated with any of the compressive mechanical properties.

All compressive mechanical properties were normally distributed except first-yield load, first-yield stiffness, and first-yield cumulative energy. All bones had substantial postyield behavior **(Figure 4)**. Sex was significantly associated with the ultimate cumulative energy and ultimate postyield energy. The mean ± SD ultimate cumulative energy for females (2,331 ± 427 N•mm) was significantly ($P = 0.05$) greater than that for males (1,567 ± 327 N•mm). Likewise, the mean ± SD ultimate postyield energy for females (809 ± 210 N•mm) was significantly ($P = 0.021$) greater than that for males (319 ± 165 N•mm).

Of the 7 bones analyzed, 4 failed because of a comminuted fracture of the proximal portion or entire length of the diaphysis (Figure 2). Three bones failed because of crushing of the proximal and distal epiphyses and metaphyses within the PMMA blocks accompanied by a longitudinal fissure (but no fracture) in the diaphysis. All 7 bones tested in compression had a first-yield point, which corresponded to metaphyseal disruption **(Figure 5)**.

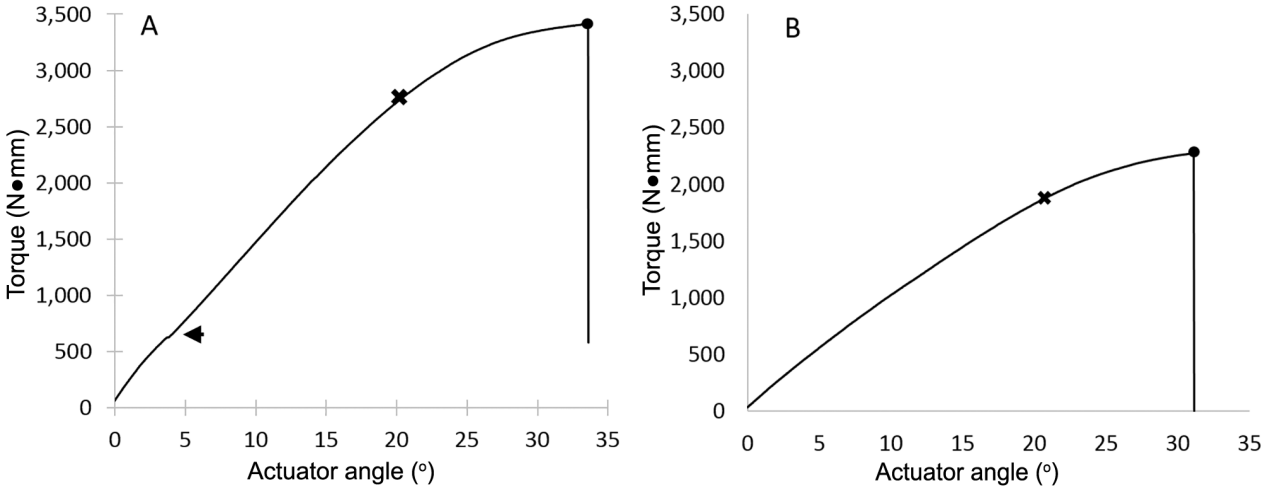

Figure 1—Representative torque-actuator angular deformation curves for 2 tibiotarsal bones of red-tailed hawks (*Buteo jamaicensis*) that underwent biomechanical testing to failure in torsion (torsional test) and did (A) and did not (B) have a first-yield point. For each of 8 birds, 1 tibiotarsal bone was randomly assigned to be biomechanically tested to failure in torsion, and the contralateral bone was assigned to be biomechanically tested to failure in compression (compression test). The proximal and distal aspects of each bone were fixed in PMMA blocks. The PMMA extended from the metaphyseal-epiphyseal junction to 1.5 cm past each end of the bone. The PMMA blocks were then mounted in a purpose-built alignment jig that was used to align the longitudinal axis of the bone with the center of rotation of a servohydraulic testing system. For the torsional test, each bone was loaded in torsion at 5°/s in external rotation under actuator displacement control and axially loaded to 5 N (approx 50% of body weight). Axial actuator displacement was held constant while the bone was externally rotated to failure, and torque and angular actuator displacement data were acquired at 128 Hz throughout the test. The first-yield point (arrow) was defined as a sharp, short decrease in torque when low torque (ie, 19% to 46% of maximum torque) was present. Four of the 8 bones tested did not have a first-yield point. The yield point (X) was defined as the first gradual deviation in curve linearity at a higher torque than that at the first-yield point (when present), and when a first-yield point was not present, it was determined by a > 1% angular deformation offset between linear regression intercepts through consecutive data points. The ultimate point (circle) was defined as the point of maximum torque. The failure point was defined as the point of the last recorded torque before bone fracture, which coincided with zero torque. All bones failed at the ultimate (maximum) torque; thus, the failure point was the same as the ultimate point.

Figure 2—Representative radiographic images of the tibiotarsal bones for one of the red-tailed hawks described in Figure 1 that were obtained after biomechanical testing to failure in torsion (A) and in compression (compression test; B). For the compression test, each bone was loaded in axial compression at 2 mm/s under actuator displacement control until the bone failed. Load and linear actuator displacement data were acquired at 128 Hz throughout the test. All bones that underwent the compression test developed a defect in the distal metaphysis (black arrow). ***See*** Figure 1 for remainder of key.

Correlation between torsional and compressive mechanical properties

The Pearson correlation coefficients and associated *P* values between torsional and compressive mechanical properties at equivalent points of the load-deformation curve were summarized **(Table 3)**. There was a significant and highly positive correlation ($r \geq 0.75$) between many of the torsional and compressive mechanical properties. However, first-yield torsional mechanical properties were not significantly correlated with the first-yield compressive mechanical properties.

Discussion

The present study was performed to evaluate the static biomechanical properties for tibiotarsal bones of red-tailed hawks. We hypothesized that the torsional and compressive properties of those bones would be positively correlated. Results of the present study indicated that there was a positive correlation between all torsional and compressive properties evaluated except displacement and cumulative energy at failure, both of which had negative, albeit insignificant, correlation coefficients. Moreover, many of the correlation coefficients were strongly positive ($r > 0.75$) and significant ($P < 0.05$). Thus, there was no evidence to justify rejection of our hypothesis. Also, although the tibiotarsal bones of this study behaved as expected in some aspects, the biomechanical test results revealed some unique mechanical behaviors.

The bones evaluated in the present study were obtained from apparently healthy adult female and male birds that lived in the wild and were euthanized because of trauma or other causes unrelated to the tibiotarsal region. The 8 birds had similar body mass (weight), and the tibiotarsal bones had similar dimensions with bilateral symmetry. Within the species, female red-tailed hawks generally have a larger body mass than males, although there is substantial overlap in the body mass ranges for females and males.[5] Of the 8 red-tailed hawks represented in the present study, only 3 were males. One of those males was extremely large, and the body mass for that bird was considered an outlier. The fact that body mass did not differ significantly between the female and male red-tailed hawks of this study was likely a function of the small number of birds and large variation in body mass. The lack of a significant difference in the mechanical properties between right and left tibiotarsal bones was expected on the basis of similar findings in other avian species.[6]

During the torsional tests, axial displacement was held constant while the bone was externally rotated, and the shortening inherent with torsion was expected to create a tensile load, or decrease compression. Interestingly, evaluation of the torsional test data revealed that all bones had an increase in axial compression instead of an increase in tension as expected. The magnitude of that increase in axial compression varied substantially (SD, 42 N) among the 8 bones. We believe this unexpected finding was a function of the anatomy of the tibiotarsal bones of red-tailed hawks. Intact bones are slightly bent so there is no pure long-axis center. Even though we did our best to align the center of rotation with the center of the bone, part of the applied rotation swept around the bone and apparently caused compression.

Evaluation of the compression test data revealed that the mean ultimate cumulative energy and postyield energy for the tibiotarsal bones of female birds were significantly greater than the corresponding means for tibiotarsal bones of male birds. The reason for this finding was unclear because bird weight and bone dimensions did not differ significantly between males and females and because sex was not significantly associated with similar torsional mechanical properties. The observed sig-

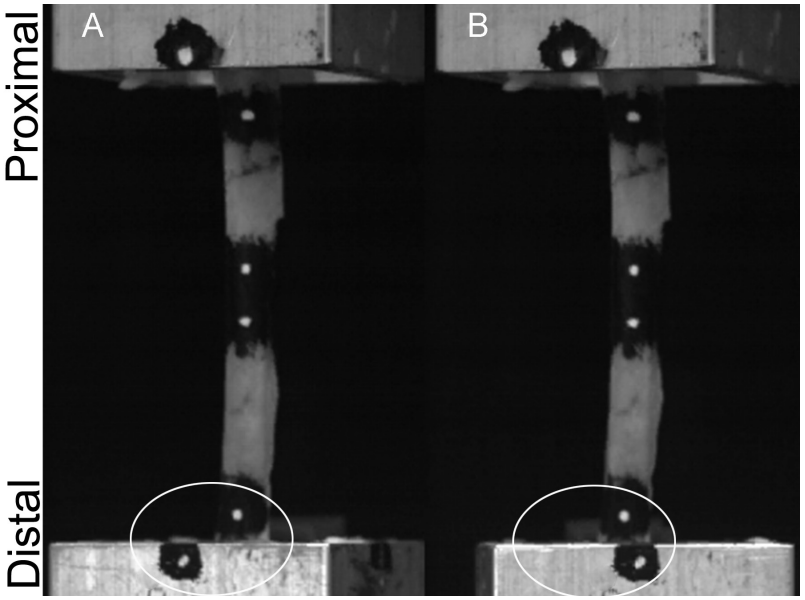

Figure 3—Video still images of a tibiotarsal bone for one of the red-tailed hawks described in Figure 1 that underwent the torsional test. The images were captured before test initiation (A) and just prior to failure (B). For all tests, video was recorded at 60 frames/s by each of 2 high-resolution (1,280 X 1,280 pixels) cameras. For the bone in this figure, white dots were painted on the diaphysis, adjacent to the proximal and distal metaphyses, and on the PMMA blocks so that motion could be tracked by a motion analysis system to better understand the local deformations that corresponded to the load-deformation data. Notice that the distal end of the bone (white oval) was rotated to the right (counterclockwise) during the test. ***See*** Figure 1 for remainder of key.

nificant differences in mechanical properties on the basis of sex might have been spurious outcomes associated with the large number of statistical comparisons performed relative to the sample size. Alternatively, it was possible that tibiotarsal cortical bone quality differed between female and male red-tailed hawks. In humans, bone quality varies between females and males, and that variation is positively associated with age.[7] Results of other avian studies indicate that, relative to males, the increased estrogen concentration of sexually mature egg-laying hens[8] and female house finches[9] and pine siskins[9] is associated with greater medullary bone density and quality. It was possible that estrogen concentration, which likely varied on the basis of the sex and age of the birds of this study, may have affected the toughness and fracture resistance of the tibiotarsal bones and contributed to the mechanical results observed. Additionally, regional variations in osteonal turnover rates within the tibiotarsal bones, as occur in the metacarpal bones of horses,[10,11] may occur in

Table 2—Dimensions and mechanical properties for tibiotarsal bones obtained from red-tailed hawks that were tested to failure in compression (compression test).

Variable	No. of bones*	Mean ± SD	Median (range)
Bone dimensions			
Diaphyseal craniocaudal diameter (mm)	7	7.1 ± 0.7	7.1 (5.8–7.8)
Diaphyseal mediolateral diameter (mm)	7	7.5 ± 0.8	7.4 (6.4–8.6)
Length (mm)	7	119.3 ± 5.1	122.2 (110.5–124.0)
First-yield point			
Displacement (mm)	7	0.29 ± 0.14	0.24 (0.13–0.56)
Load (N)	7	311 ± 103	272 (223–494)
Stiffness (N/mm)	7	1,219 ± 560	968 (661–2,297)
Cumulative energy (N•mm)	7	50.3 ± 39.0	36.8 (20.8–131.4)
Yield point			
Displacement (mm)	7	1.79 ± 0.33	1.80 (1.26–2.18)
Load (N)	7	1,585 ± 219	1,552 (1,315–1,920)
Preyield stiffness (N/mm)	7	1,053 ± 143	1,019 (862–1,211)
Cumulative energy (N•mm)	7	1,404 ± 398	1,442 (917–2,020)
Ultimate point			
Displacement (mm)	7	2.14 ± 0.37	2.29 (1.49–2.51)
Load (N)	7	1,700 ± 272	1,730 (1,389–2,109)
Postyield stiffness (N/mm)	6†	354 ± 216	285 (122–713)
Cumulative energy (N•mm)	7	2,003 ± 542	1,871 (1,221–2,620)
Postyield energy (N•mm)	7	599 ± 316	600 (162–1,009)
Failure point			
Displacement (mm)	7	9.22 ± 3.11	8.83 (5.57–15.41)
Load (N)	7	1,190 ± 190	1,210 (972–1,476)
Cumulative energy (N•mm)	7	12,157 ± 4,376	10,938 (7,809–21,331)
Postultimate energy (N•mm)	7	10,153 ± 4,562	9,718 (5,397–19,627)

Each bone was loaded in axial compression at 2 mm/s under actuator displacement control.

*Although 8 bones were tested in compression, there was a malfunction during the test for 1 bone; therefore, data from only 7 bones were analyzed. †One bone had a decrease in load between the ultimate and failure points that affected only postyield stiffness, so the datum for that bone was discarded for that variable.

See Table 1 for remainder of key.

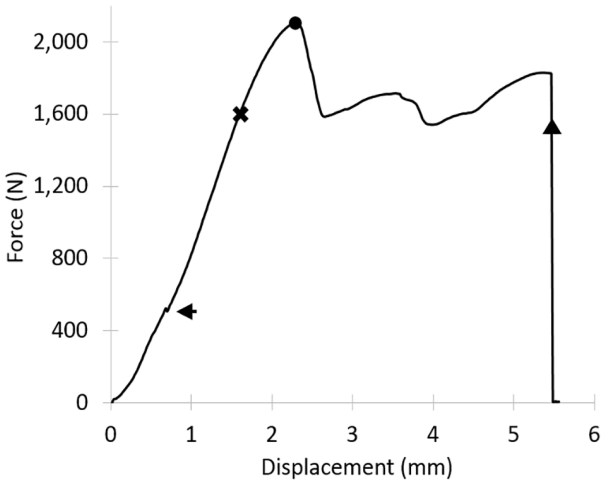

Figure 4—Representative load-displacement curve for a tibiotarsal bone for one of the red-tailed hawks described in Figure 1 that underwent the compression test described in Figure 2. The first-yield point (arrow) was defined as a sharp, short decrease in force when load was low (ie, 12% to 32% of maximum load). The yield point (X) was defined in a manner similar to that used for torsion tests, with a > 1% axial displacement offset used if a first-yield point was not present. The ultimate point (circle) was defined as the point of maximum load. The failure point (triangle) was defined as the first point after maximum load where load decreased to 70% of maximum load. For this bone, the first-yield point likely corresponded to crushing of the metaphysis within the PMMA block. ***See*** Figures 1 and 2 for remainder of key.

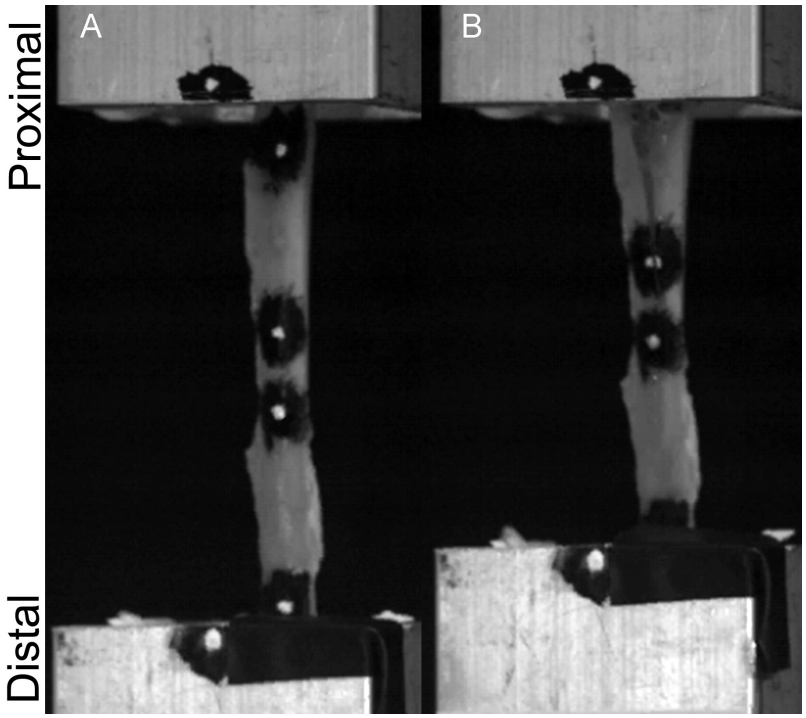

Figure 5—Video still images of a tibiotarsal bone for one of the red-tailed hawks described in Figure 1 that underwent the compression test described in Figure 2. The images were captured before test initiation (A) and at failure (B) as described in Figure 3. In panel B (relative to panel A), notice the presence of a diaphyseal fracture, disappearance of the white dots adjacent to the proximal and distal metaphyses, and shorter distance between the PMMA blocks, which reflected crushing of the proximal and distal metaphyses. ***See*** Figures 1, 2, and 3 for remainder of key.

egg-laying females and lead to regional variations in bone toughness and an increase in fatigue life. The effect of sex on the microscopic and mechanical properties of tibiotarsal bones of red-tailed hawks warrants further investigation.

Fracture configurations were consistent for bones within each test mode (torsional and compression). All bones that underwent torsional tests developed spiral diaphyseal fractures, whereas the bones that underwent compression tests developed either a comminuted diaphyseal fracture or a crushed epiphysis-metaphysis with a longitudinal diaphyseal fissure.[12] Metaphyseal disruption was observed in all bones during torsional and compression tests.

A first-yield point was identified for only 4 of the 8 bones that underwent torsional tests. Review of the videos obtained of the bones during torsional tests revealed that the first-yield point corresponded to a displacement of the distal metaphysis that exceeded the concurrent displacements of the diaphysis and proximal metaphysis for 3 of those 4 bones. The remaining bone failed at a torque that was equivalent to the torque at the first-yield point for the other 3 bones and had an incomplete spiral diaphyseal fracture that originated from the proximal metaphysis. The first-yield point for that bone was likely associated with metaphyseal disruption. It seemed unlikely that motion between the bone and PMMA or between the PMMA and machine interface led to the consistent and clear decrease in load at the first-yield point. The occurrence of a first-yield point had no significant effect on yield, ultimate, and failure torsional properties. There was also no significant difference in the dimensions of bones that did and did not have a first-yield point.

A first-yield point was detected for all bones that underwent compression tests. Review of the videos obtained of the bones during compression tests revealed that the first-yield point corresponded to large displacements of the proximal and distal metaphyses. It was not possible to determine whether metaphyseal disruption had an effect on compressive properties because all bones tested in compression had metaphyseal disruption.

The clinical relevance of the metaphyseal disruption was unknown. It is possible that the PMMA blocks caused an artificial concentration of stress in the metaphyseal region during mechanical testing that would not be present in a natural situation. Alternatively, the metaphyseal region of red-tailed hawks could be susceptible

Table 3—Pearson correlation coefficients (*r*) and associated *P* values between torsional and compressive mechanical properties at equivalent points of the load-deformation curve for the tibiotarsal bones of Tables 1 and 2.

Property	No. of paired bones	*r*	*P* value
First-yield point			
Displacement	4	0.41	0.590
Load	4	0.51	0.512
Stiffness	4	0.50	0.499
Cumulative energy	4	0.54	0.458
Yield point			
Displacement	7	0.76	0.046
Load	7	0.76	0.047
Preyield stiffness	7	0.75	0.052
Cumulative energy	7	0.52	0.235
Ultimate point			
Displacement	7	0.89	0.008
Load	7	0.85	0.016
Postyield stiffness	6†	0.90	0.037
Cumulative energy	7	0.90	0.006
Postyield energy	7	0.40	0.376
Failure point			
Displacement	7	–0.35	0.436
Load	7	0.85	0.016
Cumulative energy	7	–0.36	0.428

Each set of paired bones was obtained from the same bird. Values of $P \leq 0.05$ were considered significant. ***See*** Tables 1 and 2 for remainder of key.

to failure at fairly small loads. For the bones evaluated in the present study, metaphyseal injuries were difficult or impossible to visualize on posttest radiographs; therefore, it is plausible that metaphyseal injuries could be missed during the evaluation and treatment of fractures. Clinically, in raptors, fractures of the tibiotarsal bone generally occur 2 to 3 mm distal to the fibular crest.[2,3]

Results of the present study supported our hypothesis that the torsional properties of tibiotarsal bones in red-tailed hawks would be positively correlated with the compressive properties. When variables in torsion were compared with equivalent variables in compression, many significant associations were identified, with 56% to 81% of the variability in 1 variable being associated with the variability in the other variable. However, significant correlations were not identified between torsional and compressive properties for any first-yield variables and most cumulative energies and failure variables. The lack of a significant correlation for all failure variables except load was likely associated with differences in the nature of failure observed between torsional and compressive tests. Bones tested in torsion failed catastrophically after ultimate torque was achieved, and the absence of postultimate behavior resulted in the ultimate properties being equivalent to the failure properties. In contrast, bones tested in compression had considerable postultimate behavior before failure.

It is unknown whether the fracture configurations for the bones evaluated in the present study were more catastrophic than those observed in clinical patients. The mechanical loading conditions used in this study simulated uniaxial loads, and most bones tested had an element of comminution, which is consistent with naturally occurring tibiotarsal fractures described for raptors in another study[13] and our clinical experience. On the basis of the fracture configurations observed for the bones of this study as well as those described in clinical patients,[13] it appears that comminuted nonreconstructible fractures of the tibiotarsal bone are more common than simple load–induced fractures. Except for 3 bones tested to failure in compression, all bones tested in the present study developed fractures that involved the proximal third of the diaphysis. That region is where the bone begins to taper in a proximo-to-distal manner, and our results suggested that it may be a weak point. The location of the tibiotarsal fractures induced in the present study was consistent with the location of tibiotarsal fractures observed in red-tailed hawks examined at our institution and those of the other study,[13] which were described as midshaft fractures.

Limitations of the present study included the in vitro nature of the mechanical tests. Although torsional and compressive structural monotonic properties were determined for the bones evaluated in this study, the physiologic loading environment for tibiotarsal bones of red-tailed hawks is unknown. Fixing the ends of the bones in PMMA blocks for attachment to the mechanical testing system might have created stress at the metaphysis, which could have artificially influenced the metaphyseal disruption observed in this study. Small axial loads were likely superimposed on the torsional tests. Biaxial loading during torsional tests would have likely increased the observed torsional properties; however, results of other studies[14,15] suggest that the magnitude of those increases would have been small and insignificant. The age was unknown for the birds from which the tibiotarsal bones of this study were obtained, and age likely affected the mechanical properties of bones. Also, the effects of sex could not be separated from the effects of age. Although the number of bones evaluated in this study was small, the bones were obtained from wild birds; therefore, the sample was diverse and should have been representative of red-tailed hawks that exist in the wild.

In the present study, the mechanical properties for tibiotarsal bones of red-tailed hawks were described after those bones were tested to failure in torsion and axial compression. Fractured pelvic limbs are a major cause of morbidity and death in raptors, and elucidation of the mechanical properties of tibiotarsal bones can help clinicians formulate fracture repair options for raptors. Further experimental and clinical investigations into the mechanics of metaphyseal disruption during fracture of tibiotarsal bones in red-tailed hawks are necessary.

Acknowledgments

Supported by the Center for Companion Animal Health, School of Veterinary Medicine, University of California-Davis.

The authors declare that there were no conflicts of interest.

Footnotes

a. NEXT digital radiography system, SOUND, Carlsbad, Calif.
b. HF100/30+ x-ray generator, MinXray Inc, Northbrook, Ill.
c. Digimatic caliper, Mitutoyo America Corp, Aurora, Ill.
d. Coe tray plastic, GC America Inc, Chicago, Ill.
e. Model 809 axial-torsional testing system, MTS Systems Corp, Minneapolis, Minn.
f. SPRI, AOS Technologies AG, Baden, Switzerland.
g. VICON Motus, version 10.0, Contemplas GMBH, Kempten, Germany.
h. PROC MIXED, SAS, version 9.4, SAS Institute Inc, Cary, NC.
i. PROC CORR, SAS, version 9.4, SAS Institute Inc, Cary, NC.

References

1. Bennett RA, Kuzma AB. Fracture management in birds. *J Zoo Wildl Med* 1992;23:5–38.
2. Harcourt-Brown NH. Orthopedic conditions that affect the avian pelvic limb. *Vet Clin North Am Exot Anim Pract* 2002;5:49–81.
3. Guzman DS, Bubenik LJ, Lauer SK, et al. Repair of a coracoid luxation and a tibiotarsal fracture in a bald eagle (*Haliaeetus leucocephalus*). *J Avian Med Surg* 2007;21:188–195.
4. Redig PT. Ponder J. Orthopedic surgery. In: Samour J, ed. *Avian medicine*. 3rd ed. St Louis: Elsevier, 2016;334–343.
5. Markel MD, Sielman E, Rapoff AJ, et al. Mechanical properties of long bones in dogs. *Am J Vet Res* 1994;55:1178–1183.
6. Royal BC Museum. Avian osteology. Available at: www.royalbcmuseum.bc.ca/Natural_History/Bones/Species-Pages/RTHA.htm#Tibia. Accessed Mar 8, 2017.
7. Cole JH, van der Meulen MC. Whole bone mechanics and bone quality. *Clin Orthop Relat Res* 2011;469:2139–2149.
8. Whitehead CC. Overview of bone biology in the egg-laying hen. *Poult Sci* 2004;83:193–199.
9. Squire ME, Veglia MK, Drucker KA, et al. Estrogen levels influence medullary bone quantity and density in female house finches and pine siskins. *Gen Comp Endocrinol* 2017;246:249–257.
10. Malik CL, Stover SM, Martin RB, et al. Equine cortical bone exhibits rising R-curve fracture mechanics. *J Biomech* 2003;36:191–198.
11. Hiller LP, Stover SM, Gibson VA, et al. Osteon pullout in the equine third metacarpal bone: effects of ex vivo fatigue. *J Orthop Res* 2003;21:481–488.
12. Frankel VH, Kaplan DJ, Egol KA. Biomechanics of fractures. *J Orthop Trauma* 2016;30(suppl 2):S2–S6.
13. Bueno I, Redig PT, Rendahl AK. External skeletal fixator intramedullary pin tie-in for repair of tibiotarsal fractures in raptors: 37 cases (1995–2011). *J Am Vet Med Assoc* 2015;247:1154–1160.
14. Vashishth D, Tanner KE, Bonfield W. Fatigue of cortical bone under combined axial-torsional loading. *J Orthop Res* 2001;19:414–420.
15. Wua H-C, Xua Z, Wangb PT. Torsion test of aluminum in the large strain range. *Int J Plast* 1997;13:873–892.